Organometallic nucleophiles and Pd: What Makes $ZnMe_2$ Different? Is Au like Zn?

Juan del Pozo,[†] Estefanía Gioria,[†] Juan A. Casares,[†,*] Rosana Álvarez,[‡,*] Pablo Espinet.[†,*]

[†] IU CINQUIMA/Química Inorgánica, Facultad de Ciencias, Universidad de Valladolid, 47011Valladolid (Spain).

[‡] Departamento de Química Orgánica, Facultad de Química, Universidad de Vigo. Campus As Lagoas-Marcosende, 36310 Vigo (Spain).

Negishi, palladium, zinc, gold, metal-metal bonds, electron deficient bond, DFT calculations

ABSTRACT: The *cis*/*trans* isomerization of $[PdMeAr(PR_3)_2]$ complexes (Ar = C_6F_5, $C_6F_3Cl_2$) can take place spontaneously (via dissociation and topomerization, studied experimentally) or catalyzed by $ZnMe_2$. The later mechanism, studied by DFT methods, involves methyl exchange between Pd and Zn. The study of this catalyzed isomerization shows that, in contrast with the typical acidic behavior of Zn in ZnMeCl, Zn in $ZnMe_2$ (or, more exactly, the ZnMe bond) behaves as a strong basic center, able to attack the relatively high in energy acceptor orbital at Pd in fairly electron rich Pd complexes such as $[PdArMeL_2]$ or $[PdMe_2L_2]$. This makes the two reagents very different in Negishi couplings. The catalyzed isomerization occurs via transmetalation, thus both processes are connected. A comparison of the Pd/Zn intermediates and transition states with those found previously for Pd/Au transmetalations reveals very similar structures with intermetallic distances in the order of or noticeably shorter than the sum of the vdW radii, regardless of the nature of the metal (metallophilic Au or non metallophillic Zn). These short distances are associated to the involvement of the metals in 3c2e electron deficient bonds during R group transmetalation. In this respect there is a remarkable similarity with the structurally known behavior of main-group electron-deficient compound, which supports a unified view of the transmetalation processes.

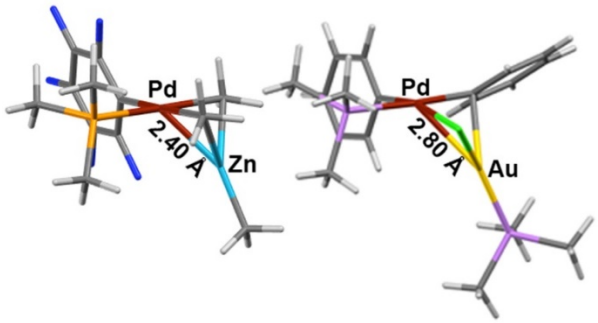

INTRODUCTION

The Negishi reaction is a powerful process for the formation of C–C bonds.[1,2] Although it is the reaction of choice for couplings involving sp^3 carbon atoms due to the high reactivity of organozinc reagents,[3,4,5] mechanistic studies on Negishi coupling have focused mainly on Ar–Ar cross-coupling,[2,6] while studies with sp^3 carbon centers are comparatively scarce.[5b,7,8,9,10] As for other palladium catalyzed couplings of organic electrophiles (R^1X) and nucleophiles (MR^2),[11] the reaction pursues the selective formation of R^1–R^2, but homocoupling byproducts, presumably formed via undesired transmetalations, frequently contaminate the reaction. For instance, formation of the so-called reduction product ArH (Ar = 2-$C_6H_4CO_2Et$) in the Negishi cross-coupling reaction of ArI and $ZnEt_2$ has been proved very recently to arise from hydrolysis of ZnArEt (formed in an undesired transmetalation) and not via β-H elimination from Pd–Et.[12] In this reaction, the "reduction" product Ar–H, the cross-coupling product Ar–Et, and the two homocoupling products Et–Et and Ar–Ar are observed, confirming active participation of isomerizations and undesired transmetalations.[13] The number and percentage of undesired products was much less when ZnEtCl was used instead of $ZnEt_2$. In order to understand this difference we decided to closely examine the behavior of $ZnMe_2$ as nucleophile towards *cis*-$[PdArMe(PPh_3)_2]$ (**1**) (Ar = $C_6Cl_2F_3$ = Rf (**1a**); Ar = C_6F_5 = Pf (**1b**)), a Pd center with relatively low electrophilicity. This kind of complex is the one from which Ar–Me cross-coupling should occur in a synthesis.

Scheme 1. A general Pd catalyzed cross-coupling cycle highlighting the existence of isomers and the importance of isomerization equilibria.

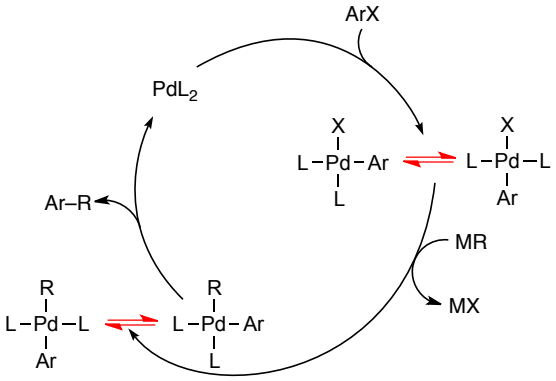

One specific question that we wanted to answer in this study is whether $ZnMe_2$ would be able to catalyze isomerization reactions of $[PdR^1R^2L_2]$ complexes. Isomerizations are important and can be determinant for the outcome of the reaction. This problem has been thoroughly discussed in the context of Stille reactions,[14] but is also operative for other cross-coupling processes. In the case studied here this isomerization might operate on the last intermediates in the cycle, preceding reductive elimination, as show in Scheme 1 where we highlight how two isomers, *cis* and *trans*, can be produced in the oxidative addi-

tion and also in the transmetalation steps of a cycle, but only the *cis* isomer can give rise to the coupling product.

The results of this investigation have revealed some interesting peculiarities of $ZnMe_2$ (and presumably $ZnEt_2$ but no other ZnR_2 with bulkier R groups) that make it very different from ZnRX (X = halide). Moreover, the transmetalation intermediates or reagents found in the calculations reveal that transmetalation and catalyzed isomerization are associated processes, and also show that the formation of short Pd–M bonds is a feature shared by Zn and Au nucleophiles.[15]

RESULTS

Non-catalyzed isomerization of trans- and cis-[PdArMe(PPh$_3$)$_2$](Ar = C$_6$F$_5$, C$_6$Cl$_2$F$_3$). The isomeric complexes *cis*-[PdArMe(PPh$_3$)$_2$] (**1**) (Ar = Rf= C$_6$Cl$_2$F$_3$(**1a**); Ar = C$_6$F$_5$ (**1b**)) and *trans*-[PdArMe(PPh$_3$)$_2$] (**2**) (Ar = C$_6$Cl$_2$F$_3$= Rf (**2a**); Ar = Pf = C$_6$F$_5$ (**2b**)) can be isolated and are sufficiently slow towards coupling to allow for monitoring of the exchange processes they undergo (Figure 1).[16]

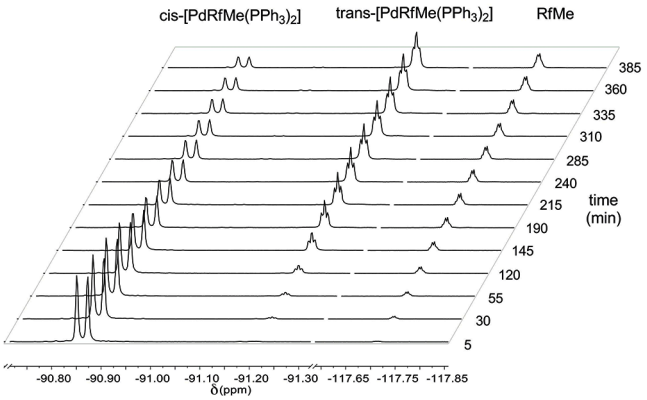

Figure 1. ^{19}F NMR spectrum (at 470.48 MHz, in THF, 25 ºC; ref. $CFCl_3$) of coupling *vs*. isomerization competence of *cis*-[PdRfMe(PPh$_3$)$_2$] (**1a**).

Starting with the *cis* isomer (**1a**), the spectrum shows that formation of the coupling product Rf–Me is slower than isomerization, but fast enough to have to consider it in the kinetic equations of isomerization. The kinetic fitting details are given as supplementary information (SI). The two complexes isomerize in THF solution at room temperature to an equilibrium with K_{eq} = 1.9 (Scheme 2).[7] This value corresponds to an energy difference of about 0.38 kcal/mol in favor of the more stable *trans* isomer. The observed rate constant of this equilibration, k_{isom}, has an inverse linear dependence on the concentration of added phosphine in the medium, indicating a two step dissociative process, shown highlighted in blue in Scheme 2, which is similar to that previously proposed for diarylpalladium complexes.[17] A rds value $\Delta G^{\ddagger}_{top}$ = 27.7 kcal/mol was found for the spontaneous isomerization, corresponding to the topomerization step in a three-coordinated intermediate. The behavior of **1b** is similar and the experimental data are almost identical (see SI).

Scheme 2. Isomerization equilibrium (black) and mechanism (blue) of cis-[PdArMe(PPh$_3$)$_2$](1) to trans-[PdArMe(PPh$_3$)$_2$](2) isomerization.

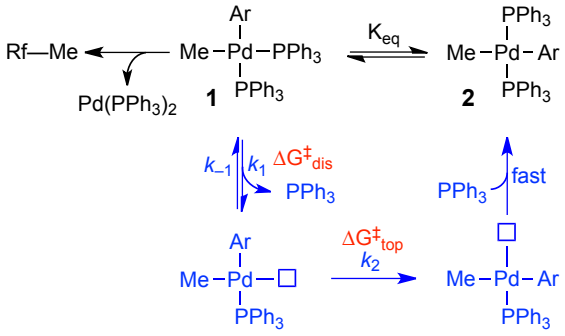

ZnMe$_2$ catalyzed isomerization of trans- and cis-[PdArMe(PPh$_3$)$_2$]. The catalyzed isomerization reaction $ZnMe_2$ + **1** = $ZnMe_2$ + **2** cannot be experimentally measured separately from the competing non-catalyzed one because, as discussed below, $ZnMe_2$ is a strong methylating reagent and its role as catalyst (in which it is not consumed) will be competing with its activity as reagent (in which it is consumed producing changes in concentration). This problem prevents to establish the reaction conditions required for experimental kinetic studies. Thus, data for the $ZnMe_2$ catalyzed isomerization pathway had to be obtained by DFT methods (wB97XD-PCM-THF/SDD-6-31G*//B3LYP/SDD-6-31G*), which afforded the interesting profile shown in Figure 2 for Ar = C$_6$F$_5$.[18]

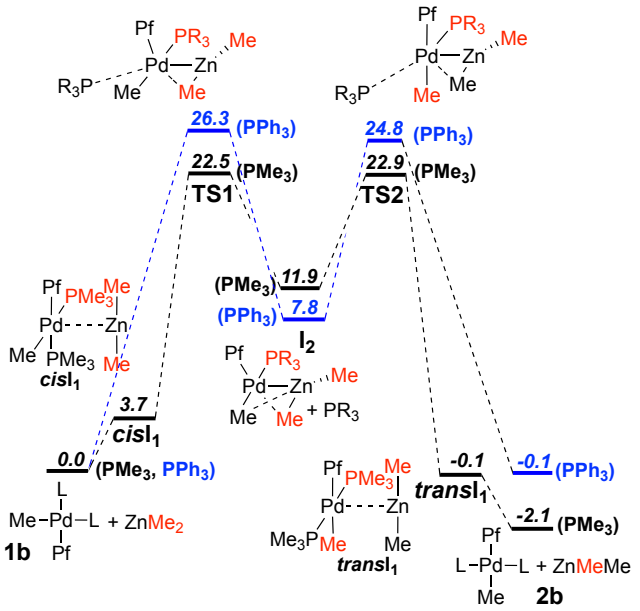

Figure 2. DFT profile of the $ZnMe_2$ catalyzed **1b**/**2b** isomerization. Gibbs energies are shown in kcal/mol (L = PMe_3, black lines; PPh_3, blue lines). NOTE: The experimental value of the equilibrium fixes the energy of **2b** in THF solution in -0.4, relative to zero for **1b**.

An examination of the profile shows that, in the catalyzed pathway, isomerization and transmetalation are directly connected (see below), as the $ZnMe_2$ catalyzed isomerization of [PdArMe(PPh$_3$)$_2$] occurs via Me/Me transmetalation. Thus this computational study of isomerization provides as well details

on the main features of a transmetalation in a system lacking typical bridging groups such as halides. The highest *catalyzed* isomerization barrier corresponds to the transmetalation on the cis complex (**1b**) and is in the order of energy (26.3 kcal/mol; note that calculations for these systems have easily 1-3 kcal/mol errors) of the experimental value for the *non-catalyzed* isomerization (27.7 kcal/mol), but still clearly higher than for transmetalations involving halides.[9,10] It is interesting to keep in mind that the $ZnMe_2$ catalyzed isomerization will follow a law $rate_{cat} = k_{cat}[ZnMe_2][Pd]$, while the uncatalyzed isomerization will follow the law $rate_{cat} = k_{uncat}[Pd]$. The total rate will be $rate_{total} = (k_{uncat} + k_{cat}[ZnMe_2])[Pd]$. For not very different isomerization barriers (k_{cat} and k_{uncat} of similar magnitude, as it is the case) the contribution of the two pathways will dramatically change depending of Pd concentration and obviously the contribution of the catalytic pathway will increase in conditions of high $ZnMe_2$ concentration ($[ZnMe_2]>>[Pd]$). This is the case of synthetic Pd catalyzed processes, where $ZnMe_2$ is used as reagent and the initial $ZnMe_2$/Pd ratio can be easily 10^2-10^3. On the contrary, for small concentrations of $ZnMe_2$ ($[ZnMe_2]<<[Pd]$), the catalyzed isomerization pathway can be slower than the uncatalyzed one.

The catalyzed isomerization process in Figure 2, from *cis* (**1b**) to *trans* (**2b**), is beautifully illustrated by sequence of structures shown in Figure 3.[19] Since the two profiles are almost symmetrical around the central intermediates $\mathbf{I_2}$, except for the change of isomer, we comment these details only for the left half of the profile.

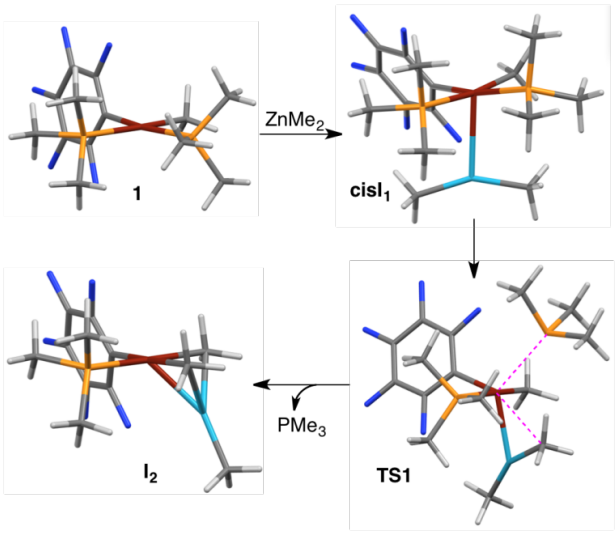

Figure 3. Snapshots of the computed $ZnMe_2$ catalyzed isomerization reaction. The structures are represented in capped stick mode using the Mercury software.[20] Color code: reddish Pd, light blue Zn, yellow-orange P, deep blue F, grey C and white H.

At the beginning of this pathway, an almost barrierless intermediate structure is observed (**cisI$_1$**) suggesting some kind of attractive interaction in the order of 3.7 kcal/mol between the two reacting molecules.[21] Particularly interesting, the transition state **TS1**, through which a phosphine substitution by one entering Me–Zn bond is taking place, shows a bipyramidal trigonal coordination for Pd, with the two apical sites occupied by one Me and one PMe_3 ligand; two of the three sites of the equatorial plane are occupied by the C_6F_5 group and the Zn atom of $ZnMe_2$; finally, the third position is in dispute between the leaving PMe_3, already at a long Pd–P distance, and one Pd–Me bond that, by this time, is already oriented towards that position (this ligand substitution is indicated by two pink dashed lines connecting the exchanging ligands to the Pd center). Increasing involvement of the Me group on Pd and eventual PMe_3 dissociation affords intermediate $\mathbf{I_2}$ where the two metals are connected by two Me bridges and a Pd–Zn bond. From that point, recoordination of the phosphine in the appropriate coordination position produces the *trans* isomer found in the calculations, **cisI$_1$–PMe$_3$**. The Pd–Zn distance in **cisI$_1$** is almost identical (2.93 Å, Table 1) to the sum of the van der Waals radii (3.02Å), which indicates a very minor interaction, perhaps still highly electrostatic in nature and associated to polarization of the electronic clouds of the metals and their ligands. This seems to be supported by the fact that this interaction does not stand changes in Pd coordination: the putative **cisI$_1$–PPh$_3$** and **transI$_1$–PPh$_3$**, bearing a more voluminous phosphine ligand, could not be computationally characterized.

Table 1. Selected geometrical parameters of the computed structures reflecting the changes in bond distances and angles along the isomerization via transmetalation. Molecule labels are as in Figure 2. Me^0 is the Me group initially on Pd. Me^1 and Me^2 are the two Me groups originally on Zn. Me–Pd and Me–Zn stand for the corresponding Csp^3–Pd or Csp^3–Zn distances.

Molecule–L	Distance (Å)* [Me^0–Pd/Me^0–Zn] {Me^2–Pd/Me^2–Zn} (Me^1–Pd/Me^1–Zn)	Distance (Å)* Zn–Pd	Me-Zn-Me largest outer angle (°)
cisI$_1$–PMe$_3$	[2.10/3.87] {3.71/1.96} (4.02/1.96)	2.93	153.6
TS$_1$–PMe$_3$	[2.09/2.95] {2.68/1.99} (4.14/1.94)	2.56	156.0
TS$_1$–PPh$_3$	[2.08/2.98] {3.08/1.96} (4.21/1.95)	2.79	156.4
I$_2$–PMe$_3$	[2.21/2.17] {2.16, 2.54} (4.23, 1.94)	2.40	146.8 123.4
I$_2$–PPh$_3$	[2.12/2.52] {2.28/2.14} (4.23/1.94)	2.42	145.8 124.6
TS$_2$–PMe$_3$	[2.12/3.13] {2.42/2.07} (4.19/1.94)	2.44	149.9
TS$_2$–PPh$_3$	[2.11/2.88] {2.72/1.98} (4.21/1.95)	2.60	153.2
transI$_1$–PMe$_3$	[2.12/3.75] {3.74/1.96} (3.93/1.96)	2.90	154.6

*For comparison Sr_{cov}(Pd+Zn) = 2.62Å; Sr_{vdW}(Pd+Zn) = 3.02Å; Sr_{cov}(Pd+Csp^3) = 2.08Å; Sr_{vdW}(Pd+Csp^3) = 3.33Å; Sr_{cov}(Zn+Csp^3) = 2.08Å; Sr_{vdW}(Zn+Csp^3) = 3.09Å.

A clear bonding interaction between the two metal fragments is found in the transition state **TS1**, where the Pd–Zn bond distances (2.56Å for PMe_3 and 2.79Å for PPh_3) are close to or shorter than the sum of covalent radii (2.62 Å).[22] Furthermore, one of the Pd–Me distances to the Me groups on Zn is much shorter (2.68Å for PMe_3 and 3.08Å for PPh_3) than the other (4.14Å for PMe_3 and 4.21Å for PPh_3), supporting engagement

in coordination to Pd of one Zn–C bond, rather than involvement of the Zn atom alone. The other Zn–Me bond of $ZnMe_2$ is an almost inactive spectator, as supported by the variation of the Zn–Me distances along the way to $\mathbf{I_2}$: one of them (Zn–Me^1 in Table 1) remains essentially unchanged along the process (1.94–1.96 Å), while the other (Zn–Me^2 in Table 1) elongates along the process of formation of the Me-bridging system (1.96–2.54 Å). In other words, what we are seeing in **TS1** is the formation of a bridging Me group involved in a 3-center 2-electron (3c2e) bonding system, at the expense of a Zn–Me bond.

In the next step of the evolution shown in Figure 3, intermediates $\mathbf{I_2}$ show the shortest Pd–Zn bonds of each series (2.40Å for PMe_3 and 2.42 Å for PPh_3), supported by two bridging Me groups. It can also be noted that the Pd–Me distances are shorter (2.16 and 2.21Å for PMe_3; 2.12 and 2.28Å for PPh_3) and the Zn–Me distances are longer (2.17 and 2.54Å for PMe_3; 2.14 and 2.52Å for PPh_3) than before or after this point in the profile;[23] furthermore, the longer Pd–Me distances are associated to the shorter Zn–Me distances in the same bridge. The largest Pd–Me distance is observed *trans* to the Pf group in $\mathbf{I_2(PPh_3)}$, but *trans* to the PMe_3 ligand in $\mathbf{I_2(PMe_3)}$, suggesting a sequence of trans influence PMe_3 > Pf > PPh_3.

A final noticeable structural change is found in the Me–Zn–Me angle, closing progressively from the initial linearity in free $ZnMe_2$ as this fragment progresses towards formation of intermediate $\mathbf{I_2}$. This reflects, in simple terms, the increasing involvement in bonding of a second p orbital of Zn (from sp towards sp^2 hybridization) as the Zn atom gets involved in more bonds. Yet, the Zn–Me distance for the terminal Me group, not involved in bridges, remains unaltered from its value in free $ZnMe_2$.

DISCUSSION

What is special in $ZnMe_2$ (or $ZnEt_2$) compared to other Zn organometallics? $ZnMe_2$ is a perfectly symmetric linear molecule (sp hybridization for Zn) in the solid state (d_{C-Zn} = 1.927(6) Å) and in the gas phase.[24] It is reluctant to coordinate OEt_2 or THF in solution, which suggests that the two strongly electron donating Me groups make, altogether, a Zn center unusually electron rich; the other potentially acceptor p orbitals of Zn, well shielded by this electron density, are high in energy and not very prone to participate in bonding, keeping the compound strictly linear coordinated except in the presence of really strong ligands.[25] For this reason the Zn center in $ZnMe_2$ does not show the acidic character found for other Zn compounds ($ZnCl_2$, ZnMeCl). Rather on the contrary, Zn in $ZnMe_2$ seems to act as a Lewis base towards the square-planar Pd acidic center. This electronic richness of the Zn center is not in contradiction with the fact that quantum mechanical calculations in the literature still support polarization of the two identical Zn–Me bonds towards their carbon ends, which develop a considerable negative atomic charge (-1.33).[26]

The Kohn-Sham orbitals shown in Figures 4 and 5 nicely support these views,[27] but also lead us to get a more accurate understanding of the initial structural considerations based only on bond distances. The HOMO1 and HOMO2 orbitals (**A**) host the four bonding electrons of $ZnMe_2$ (Figure 4) and altogether produce a high electron density in the vicinity of the Zn center. Alternatively, the equivalent orbital combinations **B** (HOMO1+HOMO 2, and HOMO2–HOMO1) allow for an easier identification of the electron density associated to the Zn–Me bond concept, and offer a more visual starting point to understand the orbital and electron density rearrangement during the evolution from $\mathbf{cisI_1}$ towards PMe_3 ligand displacement by a Zn–M bond as entering ligand.

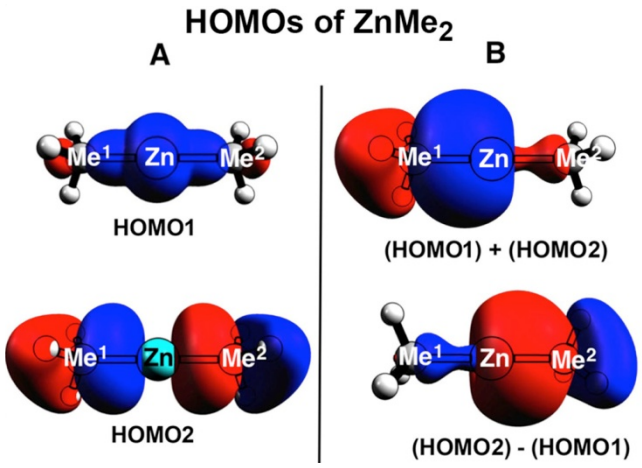

Figure 4. Selected Kohn-Sham orbitals: **A**: Molecular orbitals HOMO1 and HOMO2 for $ZnMe_2$. **B**: Alternative (HOMO2 + HOMO1) and (HOMO2 – HOMO1) combinations for $ZnMe_2$.

This evolution occurs via side-on coordination of one of the two Zn–Me bonds,[28] which eventually gets polarized towards a 3c-2e Zn-Me-Pd bond, while the other electron pair evolves to be the σ(Zn–Me) bond not involved in interaction with Pd. At the early stages of this interaction ($\mathbf{cisI_1}$) the Pd–Zn distance is still a non-bonding distance (2.95 Å, almost identical to the sum of vdW radii (3.05 Å)) but the polarization of the electron clouds of the Pd and Zn orbitals giving rise to HOMO2/Pd (Figure 5) already show that the initial contact between $ZnMe_2$ and the Pd center is beginning to create a 3c2e Pd/Zn/Me^2 interaction. In other words, the ligand substitution induced by $ZnMe_2$ occurs by nucleophilic attack of one of the two σ(Zn–Me^2) bonding electron pairs, fairly high in energy relative to the Pd acceptor orbital, which behaves as entering ligand towards an acceptor MO of the Pd complex. This empty Pd orbital is the same that receives the entering ligand in typical associative ligand substitution reactions on Pd. Meanwhile the HOMO1/Pd combination should begin to polarize slightly towards a Pd–Me^1 bonding orbital, although at this stage this can hardly be appreciated in Figure 5.[29]

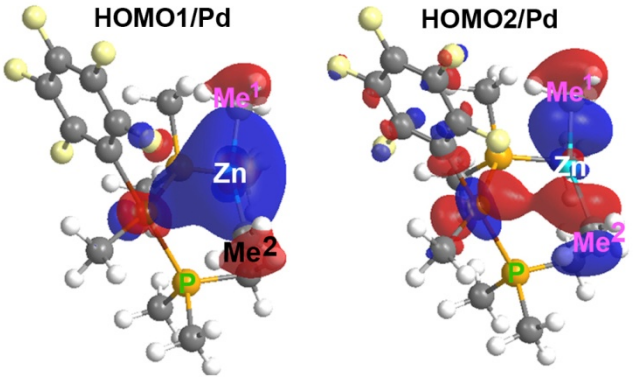

Figure 5. Selected Kohn-Sham orbitals: Incipient interactions in $\mathbf{cisI_1}$, where the molecular orbitals of the Pd/Zn adduct still let to recognize those of their $ZnMe_2$ and Pd parents.

Whereas in the conventional structural representation of Figure 3 it seems that it is the Zn center that coordinates to the Pd center, this is a naïf and misleading image as it is not the carbon or the Zn centers which are acting as the entering nucleophile, but the electron density of the bond. Figure 5 shows clearly that, from the very beginning, the interaction is defining involvement of one bond versus the other. In fact, the Pd–Me^2 is shorter than Pd–Me^1 in **cisI_1**, and Me^1 is already closer to the PR_3 ligand that will be eventually displaced via the pentacoordinated **TS1**. From that point, the implication of the two electrons of the σ(Zn–Me) bond, now fully depending on two metal centers, Zn and Pd, produces a decrease of the electron density on Zn. This stabilizes and makes more acidic the empty p orbitals on Zn, which become acceptor of electron density from the terminal Pd–Me bond, producing the second Me bridge. With these synergistic interactions, the bimetallic Pd(μ-Me)$_2$Zn molecular structure is formed.

The electron density is, as discussed, the true responsible for bond formation. This multicenter interaction is difficult to depict but, assuming the typical pictorial representation of molecular structures (based in drawing bonds as bars connecting atomic centers that share bonding electron density), we could say that the Pd coordination in **I_2** remains essentially square planar, with the two Me groups in the coordination plane and very small deviations from an ideal square plane (all angles are 90±5°), in spite of the additional Pd–Zn bond that protrudes below that plane (Figure 3). In this view the isomerization process is pivoting around the Pd–Zn bond: when the reentering PR_3 splits the Pd–Me bond *trans* to Rf, the *cis* isomer **1b** will be generated; if it splits the Pd–Me bond *trans* to the coordinated phosphine, the *trans* isomer **2b** will be formed.

For similar circumstances of other factors,[11] nucleophilic attacks occur more easily for nucleophiles with high energy HOMOs and for electrophiles with low energy LUMOs.[30] The formation of intermediate **I_2** by the mechanism discussed above is remarkable in that it occurs by nucleophilic attack to a LUMO in Pd that is not very low in energy, particularly in cases where the existence of two carbon ligands (Me and C_6F_5 in this case) makes the Pd center fairly electron rich and rises the energy of its LUMO and other orbitals. It is only the high basicity of the Zn–Me bonds in $ZnMe_2$ that makes this reaction feasible,[31] a behavior that should be less likely with ZnMeCl.

In our recent study of the Negishi cross-coupling reaction of RfI and $ZnEt_2$ to give Rf–Et,[12] already commented in the introduction, we observed that important amounts of undesired Et–Et and Rf–Et were formed at early stages of the reaction. This problem was much less visible when the reaction was carried out with ZnEtCl, and also diminished at later stages of the reaction with $ZnEt_2$ when much of the initial $ZnEt_2$ had been consumed or transformed in ZnEtCl, drastically diminishing the concentration of $ZnMe_2$ in solution. The undesired formation of Et–Et and ZnRfEt can be understood from the undesired transmetalation in equation 1, forming [$PdEt_2L_2$]:[32] The stronger nucleophile $ZnEt_2$ should be much more effective for this attack to Pd than ZnEtCl, and the more electron-rich [$PdEt_2L_2$] should be the least prone to undergo any electrophilic attack by, for instance, the byproduct ZnRfEt. Consequently, significant contribution of the exchange mechanism calculated and discussed here is expected to contibute very significantly to the undesired conversion of [$PdRfEtL_2$] to [$PdEt_2L_2$], producing undesired Et–Et homocoupling instead of Rf–Et cross-coupling.

$$PdRfEtL_2 + ZnEt_2 \rightleftharpoons PdEt_2L_2 + ZnRfEt \qquad (1)$$

For comparison we can consider transmetalations involving Pd complexes and $ZnCl_2$ or ZnRCl and see how they behave different from those with $ZnMe_2$ (Figure 6).[10] The electrophilicity of the LUMO of the relatively electron rich Pd center in [$PdMe_2L_2$] is relatively poor (two Me groups make the Pd center electron rich, as discussed before for $ZnMe_2$). On the other hand, the presence of electronegative Cl substituents that withdraw electron density from Zn stabilizes the p orbitals of Zn (as shown by the fact that complexes with THF ligands are formed). Thus the game changes: upon easy equilibrium dissociation of THF, the Zn center becomes the Lewis acid that one usually expects and, at the right of Figure 6, it is the Pd–Me bond in *trans*-[$PdMe_2L_2$] that attacks the electron poor Zn center in $ZnCl_2$. In other words, the Pd complex is now the nucleophile (through its Pd–Me bonds) and the Zn center is the electrophile. At the left of Figure 6, the reaction courses via THF displacement by a Cl ligand to make initially a Pd–Cl–Zn bridge. This makes sense because in *trans*-[$PdMeClL_2$] the electronegative Cl substituent has reduced the electron density on Pd, and the lone pairs in Cl are more nucleophilic than the Pd–Me bond with reduced nucleophilicity. In addition, a more stable non-deficient single bridged intermediate is formed.

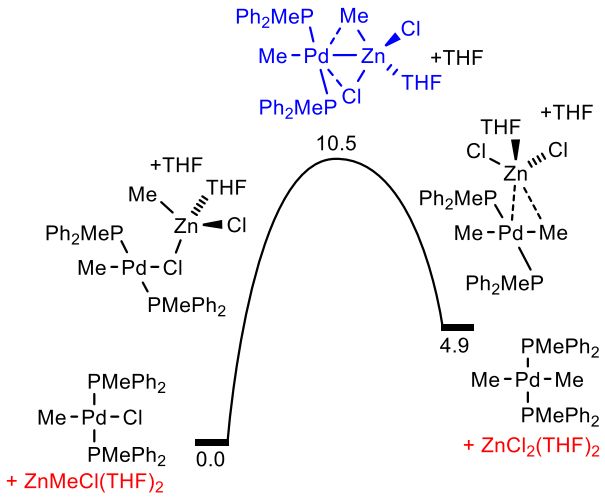

Figure 6. Transmetalation sequence calculated for the interconversion of *trans*-[$PdMeClL_2$] + ZnMeCl in *trans*-[$PdMe_2L_2$] + $ZnCl_2$. Gibbs energies in kcal/mol. See reference 10.

Is intermediate I_2 very unusual? It is only recently, on occasion of DFT mechanistic studies on transmetalations, that the surprising participation of transition-to-main group metal-metal interactions in these exchanges is being discovered. At first glance it is somewhat confusing how one should analyze the metal-metal interaction, as we are trained to consider metals as acidic centers, hence electrophilic centers. This study helps to better understand the bimetallic systems formed in transmetalations. In fact, the Me bridging interaction observed here is not as unusual as one might think at first glance: it is closely similar to the much more familiar chemical systems so often formed in the organometallic compounds of the main group metals, for instance in Al_2Me_6, where the two 3c2e

electron deficient bridges produce Me–Al and Al–Al bonding.[33] The R exchanges operating in the typical and classic Schlenk-type equilibria for main-group elements and the transmetalations operating on transition metals have much in common. Figure 7 highlights this similarity.

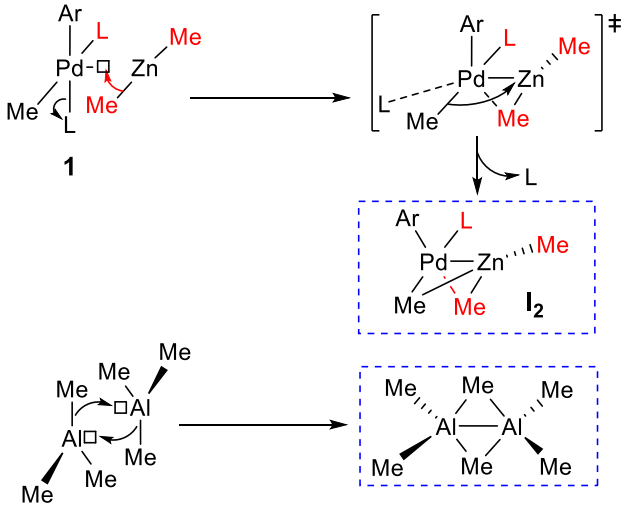

Figure 7. A comparison of the Me-bridged 3c2e bonds in Pd/ZnMe$_2$ transmetalation species and in Al_2Me_6.

Very interestingly, the isomerization mechanism observed in this paper shows also much similarity with the Rf transmetalation from *cis*-[PdRf$_2$(AsPh$_3$)$_2$] to [AuCl(AsPh$_3$)], where the Au–Cl bond displaces a ligand from Pd and the intermediates and transition states show a strong Pd–Au bond interaction (Figure 8, from right to left).[34,35,36]

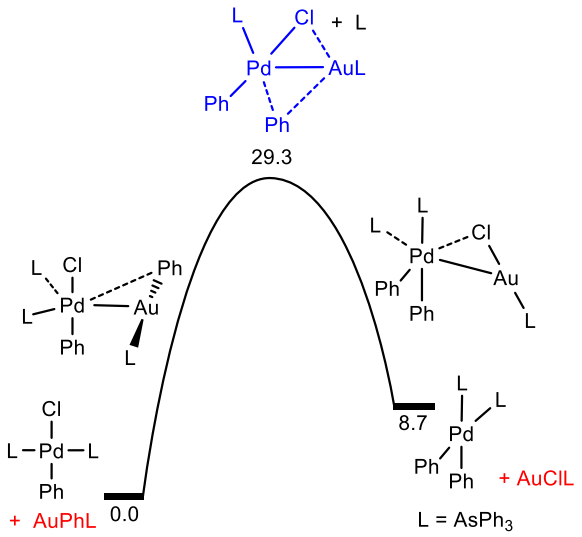

Figure 8. Calculated transmetalation sequence interconverting the systems *trans*-[PdPhClL$_2$] + AuPhL and *cis*-[PdPh$_2$L$_2$] + AuClL (Gibbs energies in kcal/mol). For details see ref. 34.

Finally, in contrast with the similar stepwise pathways for the isomerization and exchange reactions of [PdR$_2$L$_2$] with ZnR$_2$ or with AuRL (Figure 2 and Scheme 3, respectively), it is worth highlighting the differences when halides are involved, as in Figure 6 *vs*. Figure 8. Thus, at the left side of Figure 8, a moderately nucleophilic Au–Ph bond (compared to Zn–Me) is able to attack the LUMO of Pd, but in this case the Pd center bears an electronegative Cl ligand that pulls out electron density from Pd, lowers the energy of the acceptor MO, and makes Pd a stronger electrophilic center. At the right side of the transmetalation process, an Au–Cl bond leading initially to formation of a single non deficient center, at clear variance with the related reaction in Figure 6, where the nucleophile is the Pd–Me bond and the electrophile is the acidic (Cl substituted) Zn center.

Figure 9 compares the high similarity of the structure calculated here for intermediate **I$_2$** (with Zn) and that found for the case of Au. In both structures the Pd coordination is basically square planar and in both cases there is a Pd–M (M = Zn, Au) covalent bond. Some differences (angle distortion and longer Pd–M distance relative to the sum of vdW radii found in the gold system) are expected from the fact that the Au–Cl and Zn–CH$_3$ moieties differ in that Cl is larger than C and also, since Cl has electron lone pairs, the Pd–Cl–Au bridge is not electron deficient. Although ZnR$_2$ and AuRL compounds are isoelectronic, the extraordinary similarity observed is remarkable. For the gold system we first suggested the probable participation of metallophilic interactions.[37] This kind of interaction cannot be expected for light elements not submitted to relativistic effects, such as Zn and yet we find in this work that the interaction Pd–Zn is very strong. Hence our initial suggestion on the importance of metallophilic interactions in the Au/Pd system should perhaps be taken with caution, although metallophilic interactions can still be important in facilitating the initial approximation of the two metal centers. But the strong Pd–M interactions is definitely associated to the formation of 3c,2e bonds.

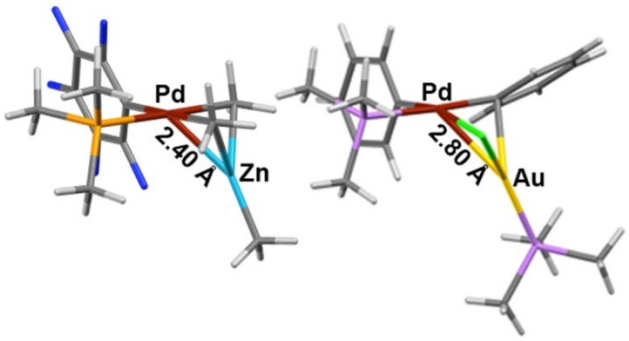

Figure 9. Structural similarity of ([(Me$_3$P)Pf**Pd**(μ-Me)$_2$**Zn**Me]) and [(Me$_3$As)Pf**Pd**(μ-Pf)(μ-Cl)**Au**(AsMe$_3$)](ref. 34). The Pd–Zn distance (2.40 Å) is noticeably shorter than the sum of vdW radii (2.62 Å). The Pd–Au distance (2.80 Å) is just a bit longer than the sum of vdW radii (2.75 Å).

It is pertinent to recall here that sixteen years ago we reported an early gold catalyzed bimetallic process, the cis/trans isomerization of [PdRf$_2$(tht)$_2$] (tht = tetrahydrothiophene), which takes minutes instead of hours when catalyzed by AuRf(tht).[38] The mechanism proposed at that time was the same depicted in Scheme 3, and it was proposed on the basis of kinetic data only. In view of the DFT data discussed above it is clear that **C** and **D** were correct but complex **D**, originally proposed as transition state, should be better considered as an intermediate totally similar to **I$_2$**, and the two Au–Rf bonds (in pink), not depicted in the original proposal, must be added.

Scheme 3. Cis-trans isomerization of [PdRf$_2$L$_2$] catalyzed by AuRfL. R^1 = R^2 = C$_6$Cl$_2$F$_3$; L = tht = tetrahydrothiophene.

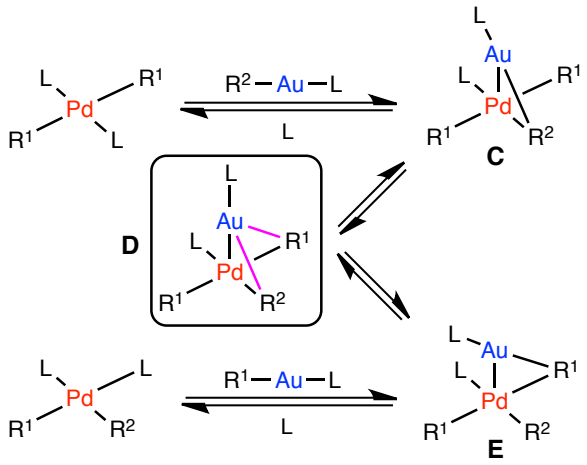

All these examples illustrate the complex interplay of electronic effects in metal compounds, which are particularly intricate for transition metal complexes, and the subtle variations of the role of a metal center as a function of its substituents. Letting aside the steric effects that strongly correct the nucleophilicity and electrophilicity values in comparison to the acidity values, Zn changes from acidic center in $ZnCl_2$ to basic in $ZnMe_2$, and the acidity of square-planar Pd^{II} complexes associated to their acceptor molecular orbitals varies importantly with the nature of the ligands.

CONCLUSIONS

$ZnMe_2$ and ZnMeCl are very different nucleophiles for the transmetalation of Me groups to Pd, and presumably to other transition metals. In the former, the metal center behaves as a basic, highly nucleophilic center and the Me–Zn bond is able to react, even with fairly electron rich Pd complexes such as [PdR$_2$L$_2$], to produce L substitution and form [LRPd(μ-Me)(μ-R)ZnMe] intermediates from which transmetalation or isomerization can follow. In contrast, the metal center at ZnMeCl is acidic and has the tendency to react, in isomerization and transmetalation reactions, via intermediates or transition states using non deficient Pd(μ-Cl)Zn bridges.

The bridged structures with at least one electron deficient component (Me, Et bridges) formed in the Pd/Au and Pd/Zn transmetalation reactions show covalent intermetallic distances noticeably shorter than the sum of the vdW radii, regardless of the possible metallophilic nature of the metal (Au) or not (Zn), because its origin is the 3c2e nature of the deficient bond. In this respect there is remarkable similarity with the behavior of main-group electron-deficient compounds.

EXPERIMENTAL SECTION

General Methods. All reactions were carried out under N_2 or Ar in THF dried using a Solvent Purification System (SPS). NMR spectra were recorded on Bruker Advance 400, Varian AV 400 or Varian AV 500 instruments equipped with variable-temperature probes. Chemical shifts are reported in ppm from tetramethylsilane (^{1}H), and CCl_3F (^{19}F), with positive shifts downfield, at ambient probe temperature unless otherwise stated. The temperature for the NMR probe was calibrated with an ethylene glycol standard.[39] In the ^{19}F and ^{31}P NMR spectra registered in non-deuterated solvents, a coaxial tube containing acetone-d$_6$ was used to maintain the lock ^{2}H signal, and the chemical shifts are reported from the CCl_3F signal in deuterated acetone. The compounds *cis*-[PdRfMe(PPh$_3$)$_2$] (**1a**) and *trans*-[PdRfMe(PPh$_3$)$_2$] (**2a**) were prepared as reported in the literature.[7] The previously unreported 1b and 2b were prepared similarly but using C_6F_5Li.

Kinetic experiments. In a standard experiment a NMR tube cooled to -10 ˚C was charged with *cis*-[PdRfMe(PPh$_3$)$_2$] (**1a**) (10 mg, 1.13x10^{-2} mmol), PPh_3 (0 to 6 mg; 0 to 2.3x10^{-2} mmol), and THF (0.60 ml). When the mixture got dissolved a coaxial capillary containing acetone-d_6 was added and the sample was placed into the NMR probe thermostated at 25 ˚C. The evolution was monitored by ^{31}P NMR or by ^{19}F NMR spectroscopy. Concentration-time data were acquired by integration of the ^{19}F NMR signals. In order to consider the reaction as irreversible and to avoid the decomposition of the starting complex to palladium (0), only data points of the first 12% of the reaction were used.

Computational methods. PMe_3 and PPh_3 were used as ligands[40] for the DFT computational study[41] (level of theory wB97XD-PCM-THF/SDD-6-31G*//B3LYP/SDD-6-31G*).[42]

ASSOCIATED CONTENT

Electronic Supplementary Information (ESI) Available: Text, figures, tables, containing experimental and kinetic details and computational information (17 pages).

AUTHOR INFORMATION

Corresponding Author

E-mail: *espinet@qi.uva.es*

E-mail: *casares@qi.uva.es*

E-mail: *rar@uvigo.es*

Notes

The authors declare no competing financial interests.

ACKNOWLEDGMENT

Financial support is gratefully acknowledged from the Junta de Castilla y León (Projects GR169 and VA256U13), and the Spanish MINECO (CTQ2013-48406-P and CTQ2012-37734). We also thank Centro de Supercomputación de Galicia (CESGA, ICTS240-2013 and ICTS257-2014) for generous allocation of computing resources. J. delPozo and E. Gioria thank Ministerio de Educación, Cultura y Deporte for FPU grants.

REFERENCES

(1) a) Negishi, E. *Angew. Chem. Int. Ed.;* **2011**, *50*, 6738–6764 (Nobel lecture). (b) *Handbook of Organopalladium Chemistry for Organic Synthesis*; Ed. by Negishi, E. Wiley-Interscience: New York, 2002; Volume 1, Part III; (c) Negishi, E.; Zeng, X.; Tan, Z.; Qian, M.; Hu, Q.; Huang, Z.; Chapter 15 in *"Metal-Catalyzed Cross-Coupling Reactions"*. Ed. by A. de Meijere, F. Diederich, Wiley-VCH. 2004.

(2) For recent reviews of Negishi reaction see: (a) Jana, R.; Pathak T. P.; Sigman, M. S.; *Chem. Rev.* **2011**, *111*, 1417–1492. (b) Wu, X.-F.; Anbarasan, P.; Neumann, H.; Beller, M.; *Angew. Chem., Int. Ed.*, **2010**, *49*, 9047–9050. (c) Valente,C.; Belowich, M. E.; Hadei, N.; Organ, M. G. *Eur. J. Org. Chem.* **2010**, 23, 4343–4354. (d) Phapale V. B.; Cárdenas D. *J. Chem. Soc. Rev.* **2009**, *38*, 1598-1607. (e) Wuertz S.; Glorius F. *Acc. Chem. Res.* **2008**, *41*, 1523-1533. (f) Fu, G. C. *Acc. Chem. Res.* **2008**, *41*, 1555-1564. (g) L. Jin, A. Lei. *Org. Biomol. Chem.*, **2012**, *10*, 6817. (h) Valente, C.; Çalimsiz, S.; Hoi, K.

H.; Mallik, D.; Sayah, M.; Organ, M. G. *Angew. Chem. Int. Ed.* **2012**, *51*, 3314–3332.

(3) Recent examples of the Negishi reaction involving the cross-coupling of sp^3 carbons with palladium catalysts: (a) Berretta, G.; Coxon, G. D.; *Tetrahedron Lett.* **2012**, *53*, 214–216. (b) Duez, S.; Steib, A. K.; Knochel, P. *Org. Lett.* **2012**, *14*, 1951-1953. (c) Duplais, C.; Krasovskiy, A.; Lipshutz, B. H.; *Organometallics* **2011**, *30*, 6090–6097. (d) Tanaka, M.; Hikawa, H.; Yokoyama, Y. *Tetrahedron* **2011**, *67*, 5897-5901. (e) Hunter, H. N.; Hadei, N.; Blagojevic, V.; Patschinski, P.; Achonduh, G. T.; Avola, S.; Bohme, D. K.; Organ M. G. *Chem. Eur. J.* **2011**, 17, 7845–7851. (f) Krasovskiy, A.; Thomé, I.; Graff, J.; Krasovskaya, V.; Konopelski, P.; Duplais, C.; Lipshutz, B. H. *Tetrahedron Lett.* **2011**, *52,* 2203–2205. (g) Zhang, Ting; Gao, Xiaodi; Wood, Harold B. *Tetrahedron Lett.* **2011**, *52*, 311–313. (h) Hadei, N.; Achonduh, G. T.; Valente, C.; Brien, C. J. O.; Organ, M. G. *Angew. Chem. Int. Ed.* **2011**, *50*, 3896–3899. (i) Nishihara, Y.; Okada, Y.; Jiao, J.; Suetsugu, M.; Lan, M.-T.; Kinoshita, M.; Iwasaki, M.; Takagi K. *Angew. Chem. Int. Ed.* **2011**, *50*, 8660 –8664. (j) Calimsiz, S.; Organ, M. G. *Chem. Commun.* **2011**, *47*, 1598-1600. (k) Bernhardt, S.; Manolikakes, G.; Kunz, T.; Knochel, P. *Angew. Chem. Int. Ed.* **2011**, *50*, 9205–9209.

(4) Reviews covering the cross-coupling of sp^3 carbon: (a) Li, H.; Seechurn, C. C. C. J.; Colacot T. J. *ACS Catal.* **2012**, *2*, 1147–1164. (b) Netherton, M. R.; Fu, G. C. *Adv. Synth. Catal.* **2004**, *346*, 1525-1532. (c) Frisch, A. C.; Beller, M. *Angew. Chem., Int. Ed.* **2005**, *44*, 674-688.

(5) (a) McCann, L. C.; Hunter, H. N.; Clyburne, J. A. C.; Organ, M. G. *Angew. Chem. Int. Ed.* **2012**, *51*, 7024–7027. (b) McCann, L. C.; Organ, M. G. *Angew. Chem. Int. Ed.* **2014**, *53*, 4386-4389, and references therein.

(6) For recent studies on the transmetalation of aryl and allylzinc see: (a) Liu, Q.; Lan, Y.; Liu, J.; Li, G.; Wu, Y. D.; Lei, A. *J. Am. Chem. Soc.*, **2009**, *131*, 10201–10210. (b) Li, J.; Jin, L.; Liu, C.; Lei, A. *Chem. Commun.* **2013**, *49*, 9615–9617. (c) Li, J.; Jin, L.; Liu, C.; Lei, A. *Org. Chem. Front.* **2014**, *1*, 50–53. (d) Yang, Y.; Mustard, T. J. L.; Cheong, P. H.-Y.; Buchwald, S. L. *Angew. Chem. Int. Ed.* **2013**, *52*, 14098–14102.

(7) Casares, J. A.; Espinet, P.; Fuentes, B.; Salas, G. *J. Am. Chem. Soc.*, **2007**, *129*, 3508–3509.

(8) (a) Chass, G. A.; O-Brien, C. J.; Hadei, N.; Kantchev, E. A. B.; Mu, W.-H.; Fang, D.-C.; Hopkinson, A. C.; Csizmadia, I. G.; Organ, M. G. *Chem. Eur. J.* **2009**, *15*, 4281–4288. (b) Organ, M. G.; Chass, G. A.; Fang, D.-C. *Synthesis*, **2008**, *17*, 2776–2797 (c) Hunter, H. N.; Hadei, N.; Blagojevic, V.; Patschinski, P.; Achonduh, G. T.; Avola, S.; Bohme, D. K.; Organ, M. G. *Chem. Eur. J.* **2011**, *17*, 7845–7851.

(9) Fuentes, B.; García-Melchor, M.; Casares, J. A.; Ujaque, G.; Lledós, A.; Maseras, F.; Espinet, P. *Chem. Eur. J.*, **2010**, *16*, 8596–8599.

(10) García-Melchor, M.; Fuentes, B.; Casares, J. A.; Ujaque, G.; Lledós, A.; Maseras, F.; Espinet, P. *J. Am. Chem. Soc.* **2011**, *133*, 13519–13526.

(11) Since we are speaking of reactivity of nucleophiles and electrophiles in a general way, the text could become cumbersome if we had to recall all the time the differences between Lewis acidity/electrophilicity and Lewis basicity/nucleophilicity. Acidity and basicity are thermodynamic concepts related to the energy of the corresponding empty or full frontier orbitals (with appropriate symmetry) in the fundamental state of the reagents and products, while electrophilicity and nucleophilicity are kinetic concepts that, in addition to the fundamental orbital acidity and basicity, can be importantly influenced by steric factors in the approach of the nucleophile to the electrophile, or by factors conditioning the energy of the transition states such as changes of the reaction mechanism (e.g. associative *vs.* dissociative), changes of the atoms involved (e.g. inert Pt *vs.* labile Pd) and others. Nucleophilicity scales (e.g. η_{Pt}) have been defined based on kinetic determinations on ligand substitution reactions, particularly in four-coordinated square-planar complexes (Pt^{II}, Au^{III}). A presentation of the topic and some seminal contributions can be found in: (a) Tobe, M. L. in *Comprehensive Coordination Chemistry*, vol. 1, p. 312. Wilkinson, G.; Gillard, R. D.; McCleverty, J. A. editors. Pergamon Press, Oxford (England), 1st Ed., 1987. (b) Belluco, U.; Cattalani, L.; Basolo, F.; Pearson, R. G.; Turco, A. *J. Am. Chem. Soc.* **1965**, *87*, 241–246. (c) Belluco, U.; Martelli, M.; Orio, A. *Inorg. Chem.* **1966**, *5*, 582–586. (d), Pearson, R. G.; Sobel, H.; Songstad, J. *J. Am. Chem. Soc.* **1968**, *90*, 319–326.

(12) Gioria, E.; Martínez-Ilarduya, J. M.; Espinet, P. *Organometallics*, **2014**, *33*, 4394–4400.

(13) Secondary transmetalations are also found in cross-coupling reactions with other nucleophiles (*e.g.* AuMeL as nucleophile). See for instance: Carrasco, D.; Pérez-Temprano, M. H.; Casares, J. A.; Espinet, P. *Organometallics*, **2014**, *33*, 3540–3545.

(14) (a) Pérez-Temprano, M. H.; Gallego, A. M.; Casares, J. A.; Espinet, P., *Organometallics*, **2011**, *30*, 611–617. (b) Cordovilla C.; Bartolomé C.; Martínez-Ilarduya, J. M.; Espinet, P. ACSCatal. DOI 10.1021/acscatal.5b00448

(15) The complete study of the Negishi reaction with $ZnMe_2$, including all the steps and other experimental investigations is in progress.

(16) In experimental mechanistic studies comparatively inert models offer the possibility to work on catalytic processes that are too fast for conventional reagents. In this respect fluorinated aryls such as $C_6F_3Cl_2$ (Rf) or C_6F_5 (Pf) are excellent models of conventional aryls. For their use in other studies and for their NMR spectroscopic features see: Espinet, P.; Albéniz, A. C.; Casares, J. A.; Martínez-Ilarduya J. M. *Coord. Chem. Rev.* **2008**, *252*, 2180–2208.

(17) Casado, A. L; Casares, J. A.; Espinet, P. *Inorg. Chem.* **1998**, *37,* 4154-4156, and references therein.

(18) Since the experimental studies show that Rf and Pf behave almost identical (see ESI), the group containing less electrons, Pf, was used in the DFT studies, but the results can also be applied to Rf, so Rf and Pf will be used indistinctly in the discussions, or referred to generically as Ar. On the other hand, we have carried out the calculations for PPh_3 and PMe_3 and the profile of the reaction includes both ligands as valuable information on how well PMe_3 performs as a model for PPh_3. These calculations also inform on the preliminary molecular interactions in **cisI$_1$** and **transI$_1$**, two states that are observed for PMe_3 but cannot be found for the corresponding more crowded PPh_3 complexes, probably because increased steric hindrance is enough to preclude their formation as intermediates. Finally, the calculated structures with PMe_3 allow for an easier observation of structural details in some figures used in this article.

(19) Represented for PMe_3 complexes for better visibility.

(20)http://www.ccdc.cam.ac.uk/Solutions/FreeSoftware/Pages/FreeMercury.aspx

(21) Taking an approximate value of 8 kcal/mol for the unfavorable entropy contribution on going from 2 molecules getting bonded to give 1 molecule, the calculated estimation of about 3.7 kcal/mol suggests an extremely weak association, whatever its nature.

(22) Note that all these bonds are somewhat longer in the more crowded **TS$_1$(PPh$_3$)** transition state as compared to **TS$_1$(PMe$_3$)**.

(23) The covalent radii of Pd and Zn are identical (1.31Å).

(24) (a) Bacsa J.; Hanke, F.; Hinley, S.; Odedra, R.; Darling, G.R; Jones, A. C.; Steiner, A. *Angew. Chem. Int. Ed.* **2011**, *50*, 11685–11687. (b) Haaland, A.; Green, J. C.; McGrady, G. S.; Downs, A. J.; Gullo, E.; Lyall, M. J.; Timberlake, J.; Tutukin, A. V.; Volden, H. W.;Østby, K.-A. *Dalton Trans.* **2003**, 4356–4366.

(25) Thus, anionic nucleophiles (e.g. RO^-, Me^-, etc.) will usually attack $ZnMe_2$, as in the formation of zincates. For neutral ligands, however, only few well defined complexes, always N-donor chelating or macrocyclic, are known: (a) O'Brien, P; Hursthouse, M. B.; Motevalli, M.; Walsh, J. R.; Jones, A. C. *J. Organomet. Chem.* **1993**, *449*, 1–8. (b) Coward, K.M.; Jones, A. C.; Steiner, A.; Bickley, J. F.; Smith, L. M.; Pemble, M. E. *Dalton Trans.***2000**, 3480–3482.

(26) Antes, I.; Frenking, G. *Organometallics* **1995**, *14*, 4263–4268.

(27) Kohn, W.; Sham, L. J. *Physical Review*, **1965**, A1133–A1138. Only qualitative use of the shape and symmetry of the orbitals is made. For usefulness and some limitations of the meaning of Kohn-Sham orbitals, see: S. Hamel, P. Duffy, M. E. Casida, D. R. Salahub,

J. Electron Spectrosc. Relat. Phenom., **2002**, *123*, 345-363, and references therein. Orbitals represented using Chemcraft (Figure 4, http://www.chemcraftprog.com/index.html) or Chemissian (Figure 5, http://www.chemissian.com).

(28) For an early proposal of side-on coordination of C–M (M = Hg) bond as the initial step of transmetallation from a metal nucleophile, and for early studies by Ingold, Reutov, and others see references in: Reutov, O. A. *Rus. Chem. Rev.* **1967**, *36*, 163–174.

(29) Since in a $[PdL_4]^{2+}$ complex with perfect D_{4h} symmetry the LUMO ($d_{x^2-y^2}$) produces zero overlap with σ-ligands approaching in the z direction, the acceptor orbital is an a_{1g} orbital with contributions of the 4s, $4p_z$, and d_{z^2} Pd atomic orbitals: *Inorganic Chemistry*, Purcell, K. F. and Kotz, J. C. W. B. Saunders Co., Philadelphia, (1977) p. 176. In this case, with much lower symmetry (C_s for the *cis* complex, C_{2h} for the *trans*), the orbital contribution of Pd to HOMO2/Pd in **cisI$_1$** contains important contributions of 4s, $3d_{z^2}$ and p orbitals with z component, and points toward the z direction. At variance with this, HOMO1/Pd contains $3d_{x^2-y^2}$ contribution instead of $3d_{z^2}$, which makes it fairly inefficient towards Pd/Zn/Me bonding.

(30) We are using LUMO for short, but we mean the lowest empty MO that has an appropriate symmetry to give rise to bond formation with the attacking full orbital of the nucleophile, which is not necessarily the LUMO if its symmetry does not provide positive overlapping.

(31) The high basicity refers to high energy of the orbitals hosting the electron density of the Zn–Me bond electron pair. The Zn–Me bond electron pair for ZnMeCl should be much lower in energy (less basic). Similar energetic considerations and behavior, including close relationship between basicity and nucleophilicity should be expected for $ZnEt_2$, but probably not for bulkier dialkyls where the high basicity might not be similarly reflected in high nucleophilicity because of steric hindrance.

(32) In that case L_2 was a chelating phosphine-(electron withdrawing olefin) ligand.

(33) The newest structural values, determined by powder neutron diffraction at 4.5 K, show an Al–Al distance of 2.700(10) Å (Al metallic radius is 125 Å). The bridging CD_3 groups adopt a staggered conformation with respect to each other in a molecule with C_{2h}symmetry, and there is no evidence in the structure for the involvement of the C–D bonds in the Al–CD_3–Al bridging bonding. See: McGrady, G. S.; Turner, J. F. C.; Ibberson, R. M.; Prager, M. *Organometallics* **2000**, *19*, 4398-4401.

(34) Pérez-Temprano, M.; Casares, J. A.; de Lera, A. R.; Álvarez, R.; Espinet, P. *Angew. Chem. Int. Ed.* **2012**, *51*, 4917–4920.

(35) delPozo, J.; Carrasco, D.; Pérez-Temprano, M. H.; García-Melchor, M.; Álvarez, R.; Casares, J. A.; Espinet, P. *Angew. Chem. Int. Ed.* **2013**, *52*, 2189–2193.

(36) Another case of Au/Pd transmetalation study, combining computational and the experimental reports on this transmetalation, can be found in: (a) Hansmann, M, M.; Pernpointner, M.; Döpp, R.; Hashmi, A. S. K. *Chem. Eur. J.* **2013**, *19*, 15290–15303. (b) Hashmi, A. S. K.; Lothschütz, C.; Döpp, R.; Rudolph, M.; Ramamurthi, T. D.; Rominger, F. *Angew. Chem. Int. Ed.* **2009**, *48*, 8243–8246. (c) Hashmi, A. S. K.; Döpp, R.; Lothschütz, C.; Rudolph, M.; Riedel, D.; Rominger, F. *Adv. Synth. Catal.* **2010**, *352*, 1307–1314.

(37) Metallophilic interactions are usually in the order of energy of weak H-bonds.

(38) Casado, A. L.; Espinet, P. *Organometallics*, **1998**, *17*, 3677-3683.

(39) Amman, C.; Meier, P.; Merbach, A. E. *J. Magn. Reson.* **1982**, *46*, 319-321.

(40) PMe_3, which was initially used as ligand because of its lower computational cost, has been widely used as model. See, for instance: (a) Fromm, A.; van Wullen, C.; Hackenberger, D.; Goossen, L. J. *J. Am. Chem. Soc.* **2014**, *136*, 10007-10023. (b) González-Pérez, A. B.; Álvarez, R.; Faza, O. N.; de Lera, A. R.; Aurrecoechea, J. M. *Organometallics*, **2012**, *31*, 2053- 2058. (c) Liu, Q.; Lan, Y.; Liu, J.; Li, G.; Wu, Y.-D.; Lei, A. *J. Am. Chem. Soc.* **2009**, *131*, 10201-102010. d) Goosen, L. J.; Koley, D. K.; Hermann, H. L.; Thiel, W. *Organometallics* **2006**, *25*, 54-67.

(41) Frisch, M. J.; Trucks, G. W.; Schlegel, H. B.; Scuseria, G. E.; Robb, M. A.; Cheeseman, J. R.; Scalmani, G.; Barone, V.; Mennucci, B.; Petersson, G. A.; Nakatsuji, H.; Caricato, M.; Li, X.; Hratchian, H. P.; Izmaylov, A. F.; Bloino, J.; Zheng, G.; Sonnenberg, J. L.; Hada, M.; Ehara, M.; Toyota, K.; Fukuda, R.; Hasegawa, J.; Ishida, M.; Nakajima, T.; Honda, Y.; Kitao, O.; Nakai, H.; Vreven, T.; Montgomery, J. A.; Peralta, J. E.; Ogliaro, F.; Bearpark, M.; Heyd, J. J.; Brothers, E.; Kudin, K. N.; Staroverov, V. N.; Kobayashi, R.; Normand, J.; Raghavachari, K.; Rendell, A.; Burant, J. C.; Iyengar, S. S.; Tomasi, J.; Cossi, M.; Rega, N.; Millam, J. M.; Klene, M.; Knox, J. E.; Cross, J. B.; Bakken, V.; Adamo, C.; Jaramillo, J.; Gomperts, R.; Stratmann, R. E.; Yazyev, O.; Austin, A. J.; Cammi, R.; Pomelli, C.; Ochterski, J. W.; Martin, R. L.; Morokuma, K.; Zakrzewski, V. G.; Voth, G. A.; Salvador, P.; Dannenberg, J. J.; Dapprich, S.; Daniels, A. D.; Farkas, O.; Foresman, J. B.; Ortiz, J. V.; Cioslowski J.; Fox, D. J. Gaussian 09, Revision B.01, Wallingford CT, **2009**.

(42) The level of theory adopted was a compromise between the quality of the theory and the time required to compute the model. On the other hand, B3LYP is a very effective density functional and it has been subjected to extensive testing. (a) Becke, A. D. *J. Chem. Phys.,* **1993**, *98*, 5648-5652. (b) Lee, C.; Yang, W.; Parr, R. G. *Phys. Rev. B.,* **1988**, *37*, 785-789. (c) Andrae, D.; Häussermann, U.; Dolg, M.; Stoll, H.; Preuss, H. *Theor. Chim. Acta.* **1990**, *77*, 123-141. The dispersion correction had been also included as single point correction to the gas energy of the optimized structures, using wB97Xd as DFT functional: Chai, J.-D.; Head-Gordon, M. *Phys. Chem. Chem. Phys.* **2008**, *10*, 6615